JACS
JOURNAL OF THE AMERICAN CHEMICAL SOCIETY

Article

pubs.acs.org/JACS

Unraveling the Enigmatic Mechanism of L-Asparaginase II with QM/QM Calculations

Diana S. Gesto, Nuno M. F. S. A. Cerqueira, Pedro A. Fernandes, and Maria J. Ramos*

Department of Chemistry, Sciences Faculty of Porto University, Porto, Portugal

Supporting Information

ABSTRACT: In this paper, we have studied the catalytic mechanism of L-asparaginase II computationally. The reaction mechanism was investigated using the ONIOM methodology. For the geometry optimization we used the B3LYP/6-31G(d):AM1 level of theory, and for the single points we used the M06-2X/6-311++G(2d,2p):M06-2X/6-31G(d) level of theory. It was demonstrated that the full mechanism involves three sequential steps and requires the nucleophilic attack of a water molecule on the substrate prior to the release of ammonia. There are three rate-limiting states, which are the reactants, the first transition state, and the last transition state. The energetic span is 20.2 kcal/mol, which is consistent with the experimental value of 16 kcal/mol. The full reaction is almost thermoneutral. The proposed catalytic mechanism involves two catalytic triads that play different roles in the reaction. The first triad, Thr12-Lys162-Asp90, acts by deprotonating a water molecule that subsequently binds to the substrate. The second triad, Thr12-Ty25-Glu283, acts by stabilizing the tetrahedral intermediate that is formed after the nucleophilic attack of the water molecule to the substrate. We have shown that a well-known Thr12-substrate covalent intermediate is not formed in the wild-type mechanism, even though our results suggest that its formation is expected in the Thr89Val mutant. These results have provided a new understanding of the catalytic mechanism of L-asparaginases that is in agreement with the available experimental data, even though it is different from all earlier proposals. This is of particular importance since this enzyme is currently used as a chemotherapeutic drug against several types of cancer and in the food industry to control the levels of acrylamide in food.

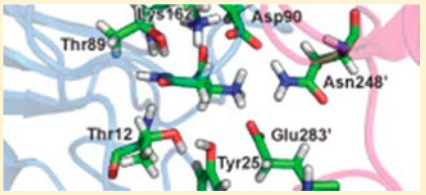

INTRODUCTION

Recent studies show that the decrease of the concentration of highly expressed amino acids in tumors can retard or even stop tumor growth without affecting the metabolism of normal cells.[1,2] The starvation of cancer cells through amino acid deprivation has thus become an encouraging strategy in cancer therapy. However, restricted diet is not enough to control the concentration of these amino acids in the blood serum. Therefore, the administration of enzymes specifically addressed to metabolize these amino acids is the method currently used. One of the therapies recently approved by the FDA to decrease amino acid blood pools is the administration of the enzyme L-asparaginase.[1]

L-Asparaginase (L-asparaginase amidohydrolase, EC 3.5.1.1) is an enzyme that hydrolyzes L-asparagine to L-aspartate, with the release of one ammonia molecule (Figure 1). It is currently used in both cancer therapy and the food industry. This enzyme is an important chemotherapeutic drug approved by the FDA and with activity against several types of cancer, such as acute lymphoblastic leukemia,[3,4] lymphosarcoma[4] and a few subtypes of non-Hodgkin's lymphoma.[5] The mechanism through which L-asparaginase destroys cancer cells is related to the fact that, in certain types of tumor, the production of asparagine synthase is limited. These cells are, therefore, incapable of producing enough amounts of asparagine to support their rapid growth, which promotes their dependence on external sources of this amino acid. The treatment with L-asparaginase reduces the levels of asparagine in the bloodstream, and since normal cells are capable of producing enough quantity of this amino acid to survive, only cancer cells will be selectively affected.[6] This means that L-asparaginase can be efficiently used to control the growth of the tumor, and eventually to destroy it, while leaving the normal cells unharmed. Although L-asparaginase has been identified in many organisms, only enzymes with bacterial origin are used in cancer therapy, and from these, only type II L-asparaginases have anticancer activity. This is due to the fact that type II bacterial L-asparaginase has greater affinity to asparagine ($KM = 1.15 \times 10^{-5}$) when compared with type I ($KM = 3.5 \times 10^{-3}$).[7] Since only L-asparaginase II shows anticancer properties, our study was mainly focused on this enzyme.[1,2] In food industry, L-asparaginase is also being used to reduce the formation of acrylamide from starchy foods.

Despite all of these current uses of L-asparaginase in medicinal and industrial applications, the reaction mechanism of this enzyme is still not known to its full extent. Taking this into account, we have studied the mechanism by computational means.

Research on L-asparaginase and related amidohydrolases has been going on for over 40 years, but the correct understanding of the catalytic mechanism remains enclosed on the available X-ray structures. In this period of time, the detailed enzymological

Received: October 15, 2012
Published: April 1, 2013

dx.doi.org/10.1021/ja310165u | J. Am. Chem. Soc. 2013, 135, 7146−7158

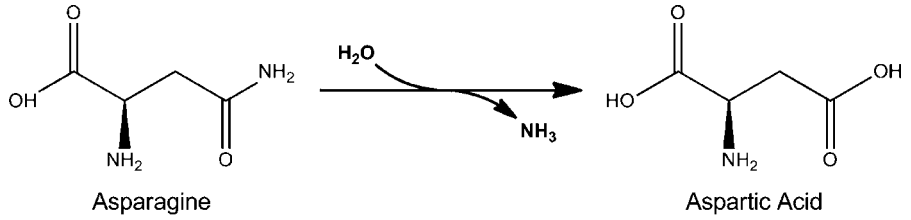

Figure 1. Reaction catalyzed by L-asparaginase.

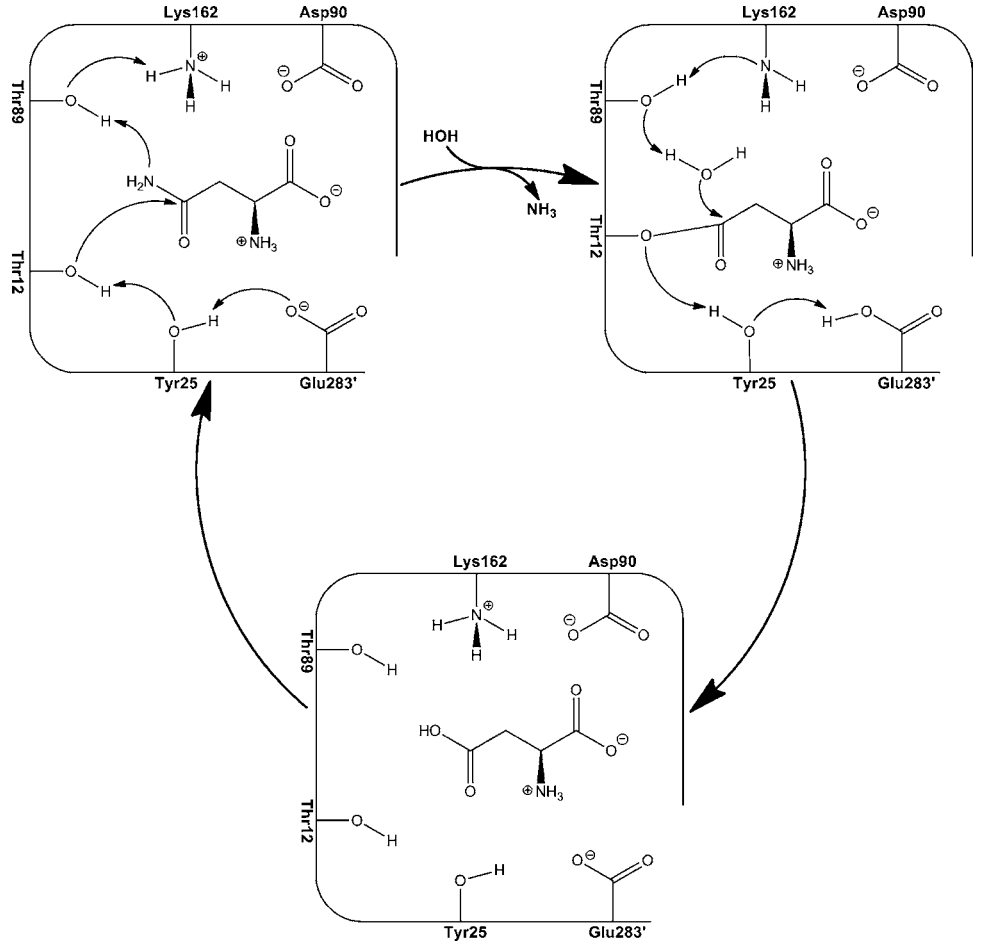

Figure 2. Currently proposed catalytic mechanism of L-asparaginase II.

study of L-asparaginases has been focused mainly on *Escherichia coli* asparaginase (EcA). However, several studies have shown that the enzymatic mechanisms of all type II amidohydrolases are very similar.

The first crystallographic model of this enzyme was that of Acinetobacter gluataminasificans glutaminase-asparaginase, reported in 1988.[8] Several crystal structures have been reported since then, some containing only the enzyme,[9,10] while others are complexes of the enzyme with other compounds such as the substrate L-asparagine, the product L-aspartate,[11,12] the alternative products D-aspartate, L-glutamate and L-succinic acid,[13] or even suicide inhibitors such as the L- and D-stereoisomers of 6-diazo-5-oxy-norleucine.[14]

Detailed analysis of the active sites of bacterial L-asparaginase II of E.coli, Erwinia carotovora and *Erwinia chrysanthemi* showed a remarkable structural conservation among L-asparaginases. The binding pocket of these enzymes involves residues from both subunits of the intimate dimer, that is, Thr12A, Tyr25A, Ser58A, Gln59A, Thr89A, Asp90A and Lys162A from one subunit (chain A), and Asn248C and Glu283C from the other subunit (chain C), that are interconnected by strong hydrogen bonds. In addition, one water molecule is structurally conserved and is part of a well-defined hydrogen-bond network (WAT1355 – PDB code 3ECA). This indicates that it is an integral part of the active-site architecture and may play a significant role in the catalytic properties of L-asparaginase.

The position of the amino acid residues in the active site suggests several possible pathways for the catalysis, but the almost symmetric location of two threonine residues, Thr12 and Thr89, above and below carbon C2 of the substrate suggests that one of them must be directly involved in the reaction.[12]

In order to decipher the involvement of these two residues in the reaction, Harms, Derst and Palm mutated these residues and evaluated the activity of the enzyme. In 1991 and 1992,

dx.doi.org/10.1021/ja310165u | J. Am. Chem. Soc. 2013, 135, 7146–7158

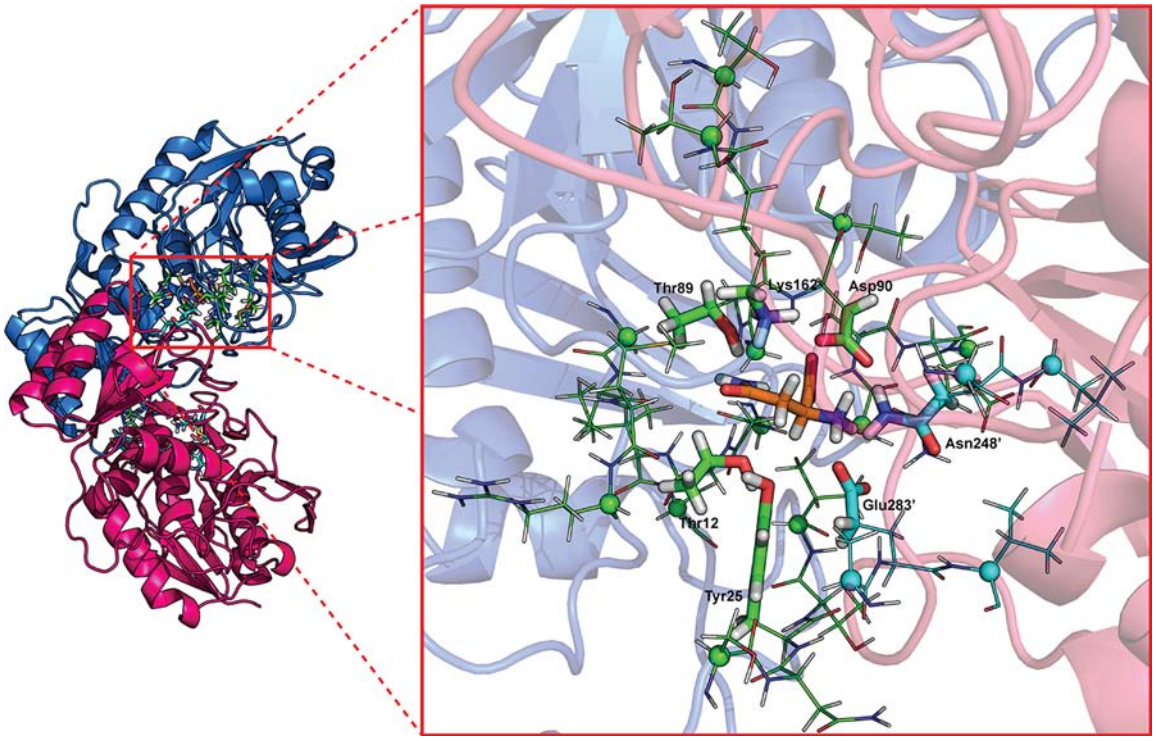

Figure 3. (Left) Cartoon representation of the L-Asparaginase II dimer (PDB ID: 3ECA), with both active sites shown in sticks. (Right) QM/QM model. The high layer is illustrated in sticks (77 atoms) and the low layer in lines (339 atoms). The frozen atoms are depicted as spheres. Carbons are colored differently for residues that belong to different subunits: green for subunit A, cyan for subunit C and orange for the substrate.

Harms[15] and Derst[16] showed that the activity of the enzyme significantly decreased when Thr12 was mutated by an alanine residue (specific activity of the mutated enzyme was less than 0.01 U/mg, against 150 U/mg for the wild type enzyme).[15] However, when it was substituted by a serine residue, no change in the enzymatic activity was observed.[16] In 1996, Palm et al. revealed that when Thr89 was mutated for a valine, the enzymatic turnover was precluded due to the formation of an acyl intermediate between Thr12 and the substrate.[17] These results seem to indicate that Thr12 plays an important role in the reaction, while Thr89 may only be needed on a subsequent step.

On the basis of these data, many authors propose that in the wild-type enzyme, the formation of an acyl-intermediate should exist and would involve the participation of Thr12. Nevertheless, the results are somewhat contradictory since, when Thr12 is mutated by an alanine, the enzyme remains active, but it is much less efficient (less than 0.01% of the specific activity of the wild-type enzyme).[15] In addition, substrate analogues have also been found covalently bound to other active site residues, such as Ser9, which is not even a conserved residue in the L-asparaginase structures.[18]

Another site-directed mutagenesis study evaluated the role of Tyr25 in the reaction. This residue, together with Thr12 and Thr89, is also conserved in all L-asparaginases and interacts very closely with Thr12 through a hydrogen bond. The idea here was to replace Tyr25 with a phenylalanine, in order to evaluate the role of the hydroxyl group of this amino acid in the reaction. The final results showed that the mutation does not have a high impact in the activity of the enzyme, and only moderately affects the KM value. Other Tyr25 mutants (Tyr-25-Ala, Tyr-25-Gly) presented similar results, suggesting that Tyr25 may not be directly involved in the reaction but may be required for the activity of the enzyme, or perhaps it might be important for the specific recognition of the native substrate.[19]

In spite of the contradictory information that all these results have generated, the currently accepted mechanism of L-asparaginases proceeds via a covalently bound enzyme intermediate as depicted in Figure 2. This implies the initial nucleophilic attack of an active site amino acid (Thr12) to the substrate (asparagine), the subsequent release of ammonia, and the formation of an acyl-enzyme intermediate, in which the substrate becomes covalently bound to the enzyme. This intermediate is then attacked by a second nucleophile, usually water, resulting in the hydrolysis of the acyl-enzyme intermediate yielding the acidic product (glutamate) and free enzyme. In this process, Lys162 has been proposed to have an active role and act as an acid and base in a proton buffer process with Thr89.

This mechanism was proposed taking into account the current knowledge about the mechanism of serine proteases that share a similar catalytic triad (Ser-Ser-Lys, instead of a Thr-Thr-Lys). Although many authors point out that the mechanism of serine proteases and L-asparaginase should be very similar, there are many other aspects that led us into thinking that they can be very different. For instance, in the mechanism of serine proteases, it is the serine residue that binds to the substrate, while in L-asparaginase it is proposed to be a threonine. Although the reactivities of threonine and serine are very similar ($pK_a \approx 13$), the presence of a methyl group nearby the hydroxyl group of threonine may difficult the formation of the acyl-enzyme intermediate. Second, even though there is an X-ray structure of L-asparaginase showing the acyl-enzyme intermediate, with Thr12 covalently bound to the substrate, this may result from an alternative reaction pathway, different from the wild-type, due to the mutation

itself. In fact, this intermediate, in which Thr12 is bound to the substrate, was exclusively obtained when Thr89 was mutated by a valine. In addition, when Thr12 is mutated by an alanine, the catalytic process is drastically reduced. However, a decrease of 1000 fold in the rate constant[16] corresponds to an increase of only 4.2 kcal/mol in the rate-limiting step. Therefore, it is not strange that the mutation of a residue at the active site, involved in the fundamental h-bond network, destabilizes the TS by 4 kcal/mol. However, that does not mean that the residue is participating directly in the reaction but instead that the residue is very close to the reactive center.

All of these results raise many questions regarding the currently accepted mechanism of L-asparaginases and therefore require an urgent re-evaluation. To this purpose, we built a model of the enzyme containing all the residues of one dimer that participate directly or indirectly in the reaction. The model used to study the catalytic mechanism of L-asparaginase II from *E. coli* was based on the X-ray structure that is available on the protein databank with the code 3ECA.[11] The structure shows that the enzyme is a tetramer composed by four identical subunits (A, B, C and D) that interact with each other in the form of two intimate pairs of subunits. In this respect the tetramer is regarded as a dimer of identical intimate dimers (here called AC and BD), each one containing two active sites that are located at the interface between both subunits. With this model we have explored many hypotheses for the catalytic mechanism and calculated accurate activation and reaction energies. The results altogether point to a catalytic pathway that is different from the earlier proposals.

METHODOLOGY

Building the Model. The model used in this study was centered in one active site of the enzyme that is located between subunit A and C. The model contains the substrate (an asparagine molecule) and Gly10, Gly11, Thr12, Ile13, Ala14, Ser23, Asn24, Tyr25, Thr26, Val27, Gly57, Ser58, Gln59, Asp60, Gly88, Thr89, Asp90, Thr91, Gly113, Ala114, Met115, Arg116, Thr161, Lys162 and Thr163, all from chain A, and Gly248, Asn248, Leu249, Ala282, Glu283 and Val284, from chain C. The model also includes one water molecule that is conserved in the active site of L-asparaginase and it is located between the substrate, Thr89 and Lys162 (Figure 3). A xyz file with the initial model is in the Supporting Information. Hydrogen atoms were added to the model using the software GaussView. Conventional protonation states for all amino acids at pH 7.0 were adopted, except for Lys162 whose side chain was kept in the form of NH_2. This protonation state was deliberately chosen because earlier experimental results have shown that Lys162 is deprotonated at neutral pH.[17] The truncation of the model was done in the terminus of each part included in the model, i.e in the carboxylate and the amino groups, which were modeled as neutral, to avoid introducing artificial charges due to the truncation process. Also, some of the residues at the terminus of each part, which did not seem to interfere with the active site, were mutated to alanine, in order to diminish the number of atoms in the model. These residues include: Val27, Arg116, Thr161, Thr163, Leu249 and Val284. The final model spans a total of 416 atoms, including all those that interact directly with the substrate and are required to maintain the main scaffold of the surrounding region of the active site as it is observed in the X-ray structure 3ECA.

Since the geometry optimizations can lead to a conformational reorganization of the terminal amino acids, and this may lead to localized unfolding in the model, we have chosen to freeze some atoms in the model in order to maintain it close to the X-ray structure. The Cα atoms that were frozen are represented in Figure 3 as spheres.

Theoretical Methods. Given that the model system is very large (over 400 atoms) and geometry optimizations are very time-consuming, we have resorted to the ONIOM methodology to perform geometry optimizations.[20,21] This method allows the division of a system in several regions, each one studied with a different theoretical level. The accuracy of the method depends on the chosen regions, the theoretical level used in each of them and the coupling scheme between the methods. According to the ONIOM methodology, we have divided the system into two overlapping layers, designated as the high-level and low-level layers. The high-level layer includes all the atoms from the substrate (asparagine) and all the residues that are directly or indirectly involved in the reaction, that is, Thr12, Tyr25, Thr89, Asp90 and Lys162 from chain A and Asn248 and Glu283 from chain C. Details about the exact atoms included (beyond the whole side chains) can be seen in Figure 3 and in the xyz file of the reactants in the Supporting Information. This layer accounts for a total of 77 atoms. The low-level layer contains all the remaining atoms of the model and has a total of 339 atoms. The atoms described at the low-level of theory do not undergo significant geometry changes during the studied reactions, but it is still important to take them into account to get the correct orientation of the active site residues and to include the medium/long-range interactions between the enzyme and the substrate. We used hydrogen atoms as link atoms to complete the valences of the bonds spanning between the two layers.

The geometry of the high-level layer was optimized with the higher theoretical level (DFT). The B3LYP functional was chosen, since it is known to give very good results for organic molecules.[22−25] The 6-31G(d) basis set was employed, as implemented in Gaussian 09.[26] The inclusion of diffuse functions in the basis set for geometry optimizations was investigated before.[27] The conclusion was that the corrections to the geometry were very small, and corrections in energy differences (such as energy barriers or energies of reaction) were negligible upon the calculation of single point energies with a more complete basis set. Therefore, it seems inadequate from a computational point of view to include diffuse functions in geometry optimizations, considering the inherent increase in computing time that they would cause. The low-level layer was treated with the semiempirical method AM1.[28]

The model, with the aforementioned constrains, was fully optimized with the Gaussian 09 standard parameters. Subsequently, several hypotheses for the reaction mechanism were explored through linear transit scans along the reaction coordinates implicated in each studied reaction. The transition states were subsequently fully geometry-optimized, starting from the structure of the higher energy point of the scans. The reactants and the products, associated with it, were determined through internal reaction coordinate (IRC) calculations. The transition state structures were all verified by vibrational frequency calculations, having exactly one imaginary frequency with the correct transition vector, even using frozen atoms, which shows that the frozen atoms were almost free from steric strain.

The energies of the minima and transition states were additionally calculated at the M06-2X/6-311++G(2d,2p) level in the high layer and M06-2X/6-31G(d) level in the low layer.[29] These single point calculations also accounted for the long-range contribution of the remaining enzyme through the inclusion of dielectric continuum (IEF-PCM), as implemented in Gaussian 09.[30] This feature is of particular importance to the study of enzymatic catalysis because the use of a continuum model is normally taken as an approximation to the effect of the long-range global enzyme environment in a reaction. A dielectric constant of $\varepsilon = 4$ was chosen to describe the protein environment of the active site in agreement with previous suggestions.[31,32] Anyway, the effect of the continuum is quite insensitive to the precise choice of the value for the dielectric constant.

The atomic charges distributions were calculated at the B3LYP level employing a Mulliken population analysis scheme, using the 6-31G(d) basis set.

The MD simulation were performed with the Amber software in the NPT ensemble (parm99 force field, 5 ns, 310.15 K, 1 bar, time step of 2 fs, bonds between H and heavy atoms frozen with the SHAKE algorithm, Coulombic forces calculated with the PME method, cutoff of 12).

Table 1. Distances Involving Some Residues of the Active Site of L-Asparaginase, the Substrate, and a Conserved Water Molecule.[a]

	distances (Å)				
	Lys162(N)-Wat(O)	Sub(C6)-Wat(O)	Asp90(O1)-Wat(O)	Asp90(O1)-Sub(C6)	Asp90(O1)- Lys162(N)
X-ray Structure 3ECA	3.7	4.8	2.5	4.2	2.6
MD Model	3.3 ± 0.6	3.9 ± 0.4	3.6 ± 1.1	4.3 ± 0.5	3.2 ± 0.9
QM/QM Model	2.8	3.8	5.3	5.2	3.1

[a]Distances were retrieved from the X-ray structure with the PDB code 3ECA, the MD molecular dynamic simulation and in the QM/QM model.

RESULTS AND DISCUSSION

In order to study the catalytic mechanism of the L-asparaginases by computational means, we based our study on the X-ray structure that is available in the protein databank with the code 3ECA.[11] As this X-ray structure has the product of the reaction bound to the active site, we first substituted the carboxylic group of the side chain of the acidic glutamate (product of the reaction) by an amide group in order to obtain the substrate asparagine (the reactant of the reaction). To evaluate if this exchange of substrates could lead to any significant conformational rearrangements in the active site, we first conducted a molecular dynamic simulation of 5 ns. The simulation included one dimer of the protein (subunit A and C from the pdb file 3ECA), the substrate (asparagine) and the solvent. The simulation revealed that the active site is very robust and most of the interactions between the active site residues were kept. The most perceptible change involved a water molecule that in the beginning of the simulation was very close to Lys162 and Asp90 and with which it interacted by two hydrogen bonds. After 2 ns, it moved closer to the substrate and retained that position till the end of the simulation (2 Å away from the previous position). When we built the QM/QM model we choose to keep the last position of the water molecule because it is more realistic than the position that it occupies in the X-ray structure 3ECA (that contains the product of the reaction bounded in the active site). The final QM/QM model was then optimized using the ONIOM hybrid methodology. Comparing with the X-ray structure 3ECA with optimized QM/QM model we can see that most of the interactions present in the region of the active site are kept almost unchanged apart from the position of one water molecule that now interacts very closely with the substrate (Table 1).

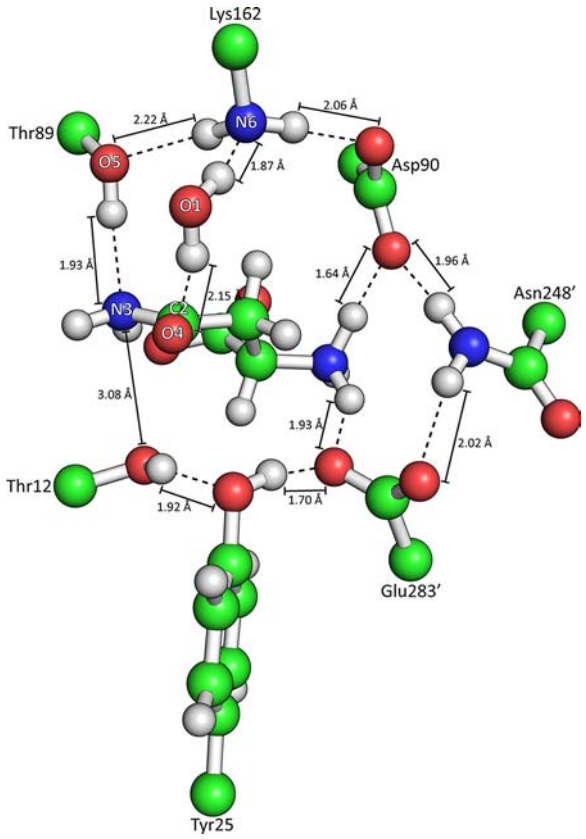

Figure 4. Optimized structure of the reactants of the reaction. For clarity, only some of the high level atoms are shown.

The optimized geometry of the QM/QM model revealed that the substrate is wrapped in a net of hydrogen bonds provided by several residues of the active site, similarly to what is observed in the X-ray structure 3ECA (Table 1) (Figure 4). In such state, the amide group of the substrate becomes constrained between Thr89 (1.93 Å) and Thr12 (3.08 Å), forcing it to acquire a planar shape, perpendicular to the side-chains of those amino acids. Such configuration is reinforced by the presence of a water molecule (WAT) that interacts very closely with the carbonyl of the amide group (2.15 Å). The position adopted by WAT and Thr89 is very important to this end and it is ensured by the conserved Lys162 that interacts very closely with both of them by two hydrogen bonds (Lys162-Thr89: 2.22 Å, Lys162- WAT: 1.87 Å). The central role of Lys162 in these interactions is only possible due to the neighbor Asp90 (2.06 Å) that behaves almost as an anchor to Lys162 and maintains its position in the active site. Asp90 also interacts with the amino group of the substrate (1.64 Å), and with Asn248 (1.96 Å) reinforcing the net of hydrogen bonds in the active site.

Thr12 lies in the bottom part of the active site and, together with Thr89 and WAT, interacts very closely with the amide group of the substrate. However, contrarily to what happens with Thr89, Thr12 does not establish a hydrogen bond with the atoms of the amide group. Instead the oxygen from the hydroxyl group points toward carbon C2, which has been proposed to be involved in the formation of the acyl-enzyme intermediate (3.08 Å). This configuration is favored by the proximity of the conserved Tyr25 that orients the hydroxyl group in its direction (1.92 Å) and by Glu283 that forces Tyr25 to occupy such position (1.70 Å). In the same way to what happens with Asp90, Glu283 also interacts with the amino group of the substrate (1.93 Å) and with Asn248 (2.02 Å). These interactions seem to be important for the correct alignment of all the residues of the active site and, at the same time, to force the substrate to acquire a specific conformation that might be required to start the reaction.

In our first attempts to study the catalytic mechanism of L-asparaginase, we tried to follow all the possible pathways that could lead to the formation of the acyl-enzyme intermediate

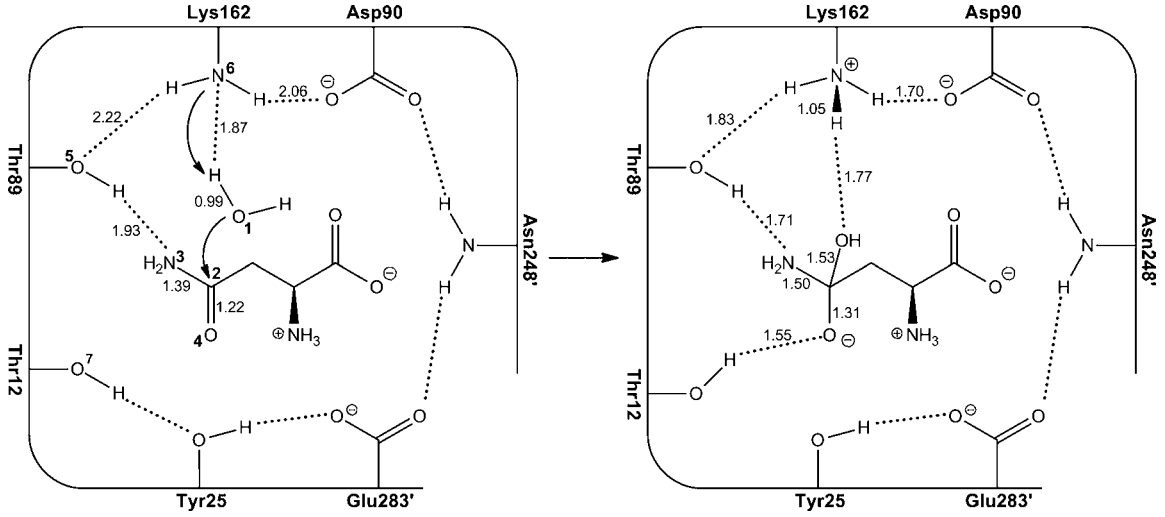

Figure 5. First step of the catalytic mechanism of L-asparaginase II.

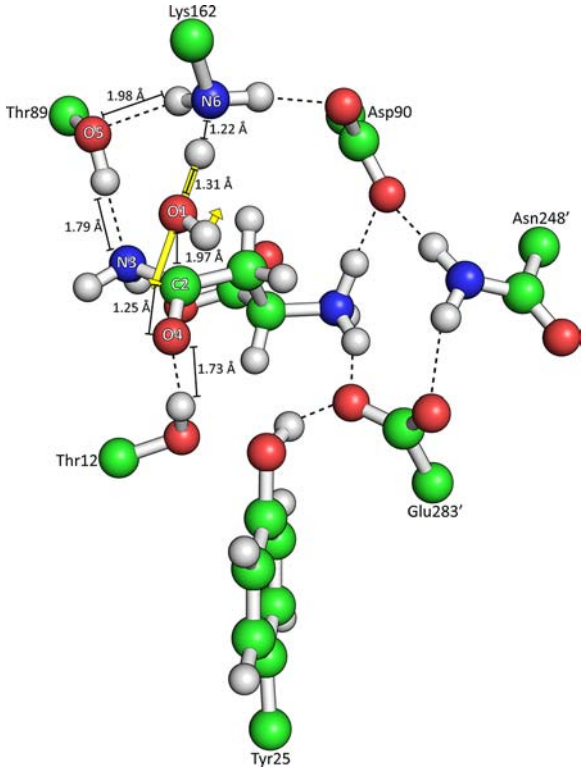

Figure 6. Transition state from the first step of the reaction mechanism of L-asparaginase II. The main vectors are represented with yellow arrows (749.3018i). For clarity, only some of the high level atoms are shown.

involving Thr12 as it is found in the mutated X-ray structure 4ECA.[17] We have located such intermediate 11 kcal/mol above the initial reactants of the wild type enzyme. The overall barrier to reach the acyl-enzyme intermediate was 25 kcal/mol in the wild-type enzyme, obtained using B3LYP/6-31G(d):AM1. However, any attempt to progress further from the intermediate always involved barriers over 50 kcal/mol. This means that this pathway is definitely not viable in the wild type enzyme. In any case it is important to note that these results do not contradict the experimental findings. Contrarily, they give us a plausible explanation for the experimental trapping of the covalently bound intermediate in the Thr89Val mutant structure because they show us that it is possible to form the covalent intermediate (assuming that its formation would have a comparable activation energy in the mutant and a smaller reaction energy) but that it is not possible to progress further from the covalent intermediate toward the final products.

Facing these results, we move forward in exploring other pathways that could be more feasible from the energetic point of view. In this process, we found that the most favorable pathway involves the nucleophilic attack of the substrate by a water molecule, and this occurs prior to the release of ammonia, contrary to what has been proposed so far in the literature.

Step 1 – Nucleophilic Attack of the Water Molecule. The water molecule that attacks the substrate in our proposal is conserved in many X-ray structures that are available in the protein databank.[11] In those structures, this molecule is trapped between Lys162, Asp90 and the substrate. In the optimized geometry of the complex that was built for this study, the water molecule is deviated by about 2 Å from the one seen in the X-ray structure 3ECA. This position was chosen based on a 5 ns molecular dynamics simulation, where we have seen that, after transforming the product present in the crystal into the substrate, the water molecule moves to a position close to one shown in Figure 4. In this new position it makes a hydrogen bond with Lys162 (1.87 Å) and is particularly close to carbon C2 of the substrate that has been proposed to be involved in the formation of the acyl-enzyme intermediate (3.06 Å) (Figure 5). Such interaction is favored by the position of the amide group of the substrate that is stabilized by the network of hydrogen bonds that are available on the active site and provides a close contact, almost free of steric hindrance.

As the reaction moves from the reactants to the products, carbon C2 changes the hybridization from sp2 to sp3, as the water molecule approaches it. Simultaneously, Lys162 becomes positively charged (−0.01 au in the reactants and 0.70 au in the products, for the $-NH_3$ group). At the transition state, the OH bond of the water molecule is elongated to 1.31 Å, the proton-nitrogen distance is 1.22 Å and the water oxygen-C2 distance is 1.97 Å. Additionally, the bond between oxygen O4 and carbon C2 elongates (1.25 Å), as it changes from a double to a single bond and the oxygen becomes negatively charged. Thr12 starts moving away from Tyr25 toward this oxygen, in order to

dx.doi.org/10.1021/ja310165u | J. Am. Chem. Soc. 2013, 135, 7146−7158

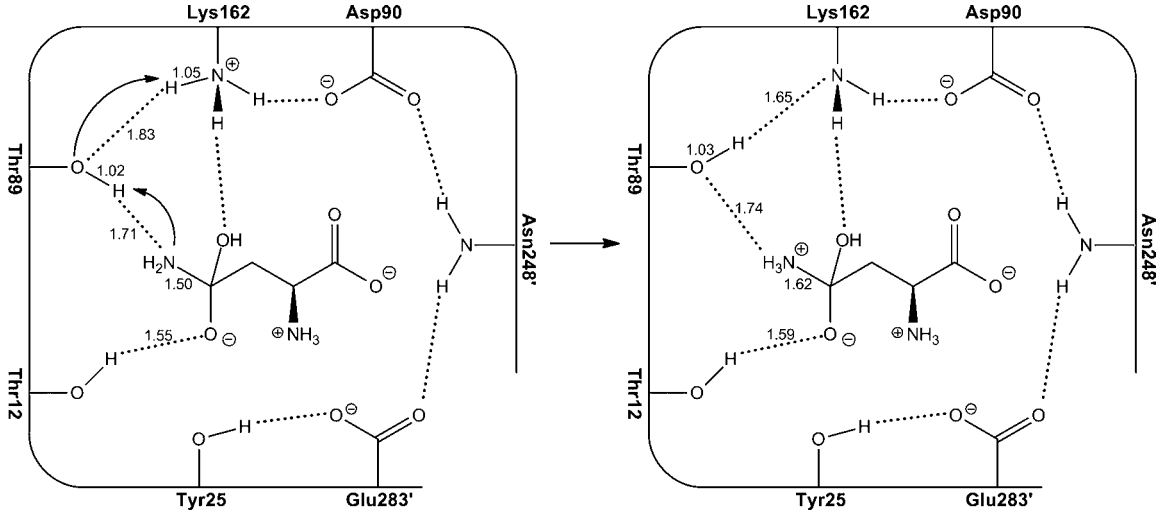

Figure 7. Second step of the catalytic mechanism of L-asparaginase.

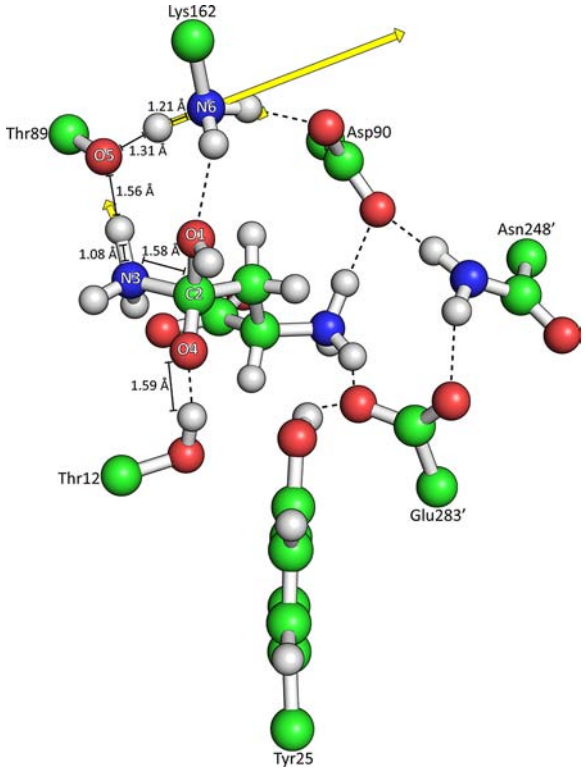

Figure 8. Transition state from the second step of the reaction mechanism of L-asparaginase II. The main vectors are represented with yellow arrows (515.8669i). (For clarity, only some of the high level atoms are shown.).

stabilize this charge (Figure 6). The transition state of this reaction is characterized by one imaginary frequency at 749 icm^{-1} and reveals that the proton transfer from the water to Lys162 occurs simultaneously with the nucleophilic attack of the water molecule to carbon C2 of the substrate.

At the end of this reaction, carbon C2 adopts a tetrahedral configuration and the hydroxyl group of the water molecule becomes covalently bound to it (Figure 5). The double bond between C2 and O4 changes to a partial single bond (distance changes from 1.22 Å in the reactants to 1.31 Å in the products) and oxygen O4 becomes negatively charged (−0.72 au). This charge is promptly stabilized by Thr12, which makes a hydrogen bond with it (1.55 Å). In the course of this reaction, the distance between carbon C2 and the amino group increases from 1.39 to 1.50 Å and the hydrogen bond between the latter and Thr89 decreases from 1.93 to 1.71 Å. The same pattern is also observed with the hydrogen bond between Thr89 and Lys162, which decreases from 2.22 to 1.83 Å due to the strengthening of the Lys162-Thr89 H bond that changes from dipolar to ionic. All of these patterns clearly indicate that the active site is ready to catalyze the proton transfer from the positively charged Lys162 to the amino group that is attached to carbon C2 of the substrate in the next step.

It should be emphasized that the role of Lys162 in step 1 is very important. Apart from being directly involved in the reaction, it guarantees the correct orientation and alignment of the water molecule as well as that of Thr89, which will be required for the next step. In addition, at the end of this reaction Lys162 becomes positively charged and interacts very closely with the anionic Asp90 (1.70 Å).

The reaction involved in step 1 has an activation energy of 20.2 kcal/mol and the reaction is endothermic (11.0 kcal/mol). In spite of high, the activation energy is still acceptable when compared with the experimental value regarding the kinetics of L-asparaginases (around 16 kcal/mol). The relatively high activation energy of this reaction may be explained, at least partially, by suboptimal position of the water molecule to perform the nucleophilic attack, as well as by the position of Thr12 which must break its hydrogen bond with Tyr25 in order to stabilize the nascent oxoanion in the substrate. The inclusion of a water molecule between Tyr25 and Thr12 might lower the barrier significantly. We have seen that such water molecule makes a hydrogen bond with the carbonyl oxygen of the substrate already in the reactants. However, we decided not to include it in the final calculations because we are unsure if that water should be present in physical conditions. The position, and particularly, the orientation of the water molecule is very important for the success of the reaction, as well as for the stabilization provided by Thr12 to oxygen O4. Other factors such as long-range interactions from the missing part of the enzyme or conformational/dynamic effects, as well as the limited accuracy of DFT, may be responsible for the small difference of 4 kcal/mol between theory and experiments.

dx.doi.org/10.1021/ja310165u | J. Am. Chem. Soc. 2013, 135, 7146−7158

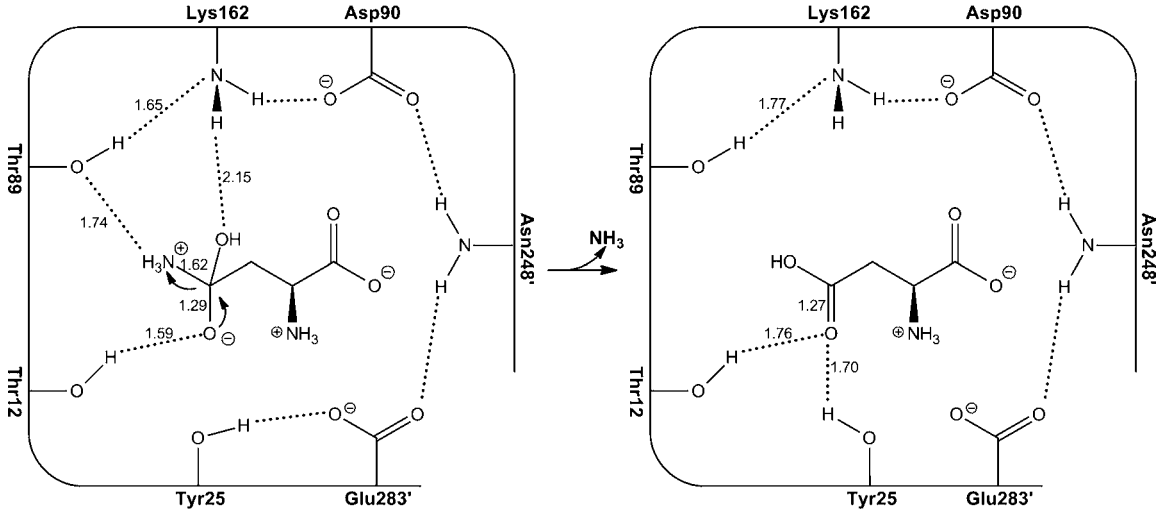

Figure 9. Third step of the catalytic mechanism of L-asparaginase.

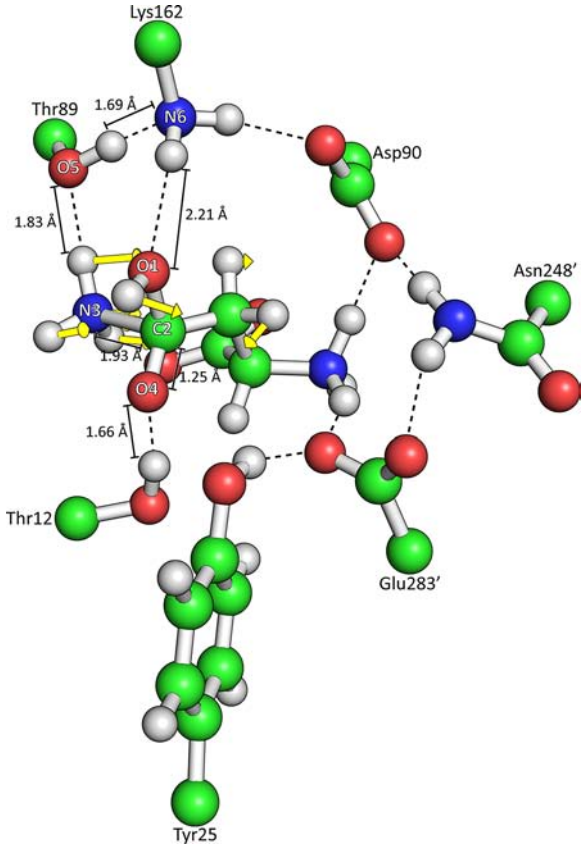

Figure 10. Transition state from the third and last step of the reaction mechanism of L-asparaginase II. The main vectors are represented with yellow arrows (−179.4042i). For clarity, only some of the high level atoms are shown.

Step 2 – Formation of Ammonia. As mentioned before, all the active site residues are preorganized to facilitate the formation of ammonia. Thr89 makes two hydrogen bonds, one with the amino group of the substrate (1.71 Å) and another with Lys162 (1.83 Å), favoring in this way the concomitant transfer of both protons (from Thr89 to the amide group and from Lys162 to Thr89) that ultimately leads to the protonation and release of the amino group attached to carbon C2 of the substrate (Figure 7). Thr12 performs a hydrogen bond with oxygen O4 and Lys162 interacts in the same way with oxygen O1, which belonged to the water molecule and is now covalently bounded to carbon C2.

As the reaction proceeds, the hydrogen from Thr89 moves to the nitrogen N3 of the amide group of the substrate in order to form the ammonia molecule. At the same time, the hydrogen from Lys162 draws closer to the oxygen from Thr89. In the transition state (Figure 8), it is possible to observe that the proton of Lys162 is halfway through to Thr89 (the distance from nitrogen N6 to the hydrogen is 1.21 Å while that of the hydrogen to the oxygen O5 is 1.31 Å). In the same way, the distance between the hydrogen from Thr89 and O5 has increased from 1.02 Å in the reactants to 1.56 Å in the transition state, while the distance between this hydrogen to nitrogen N3 has decreased to 1.08 Å. The transition state of this double proton transfer is characterized by an imaginary frequency at 515 icm^{-1}, and reveals that both protons are transferred simultaneously with a relatively low activation barrier (3.5 kcal/mol), as it was proposed before.

In the product of the reaction, one ammonia molecule is obtained but it does not unbind from the substrate, as it was expected. Instead, this group remains very weakly bounded to carbon C2 of the substrate (1.62 Å). This may explain why the reaction is endothermic by 4.9 kcal/mol. The total charge of the NH_3 group is 0.33 au and not zero because it is still bound to the substrate. One cause for such behavior may be related to the ionic bond between oxygen O4 and Thr12 (1.59 Å) that helps stabilize the tetrahedral intermediate centered on carbon C2, and will be transformed into a weaker dipolar hydrogen bond upon release of ammonia. It is also observable that the proton from Lys162 is now bound to Thr89 (distance between N6 and the proton in the products is 1.65 Å and the distance between the same proton and O5 is 1.03 Å).

It is also interesting to note that the structure of the reactants, transition state and products can be almost superimposed with a root means square deviation of 0.3 Å, considering only the QM region. This means that the active-site is extremely well preorganized to move from the reactants to the transition state and to the products, with minimal reorganization energetic cost. In this regard, the positions occupied by Thr89 and Lys162 are very important but also that of Thr12, which continues to stabilize the negatively charged

dx.doi.org/10.1021/ja310165u | J. Am. Chem. Soc. 2013, 135, 7146−7158

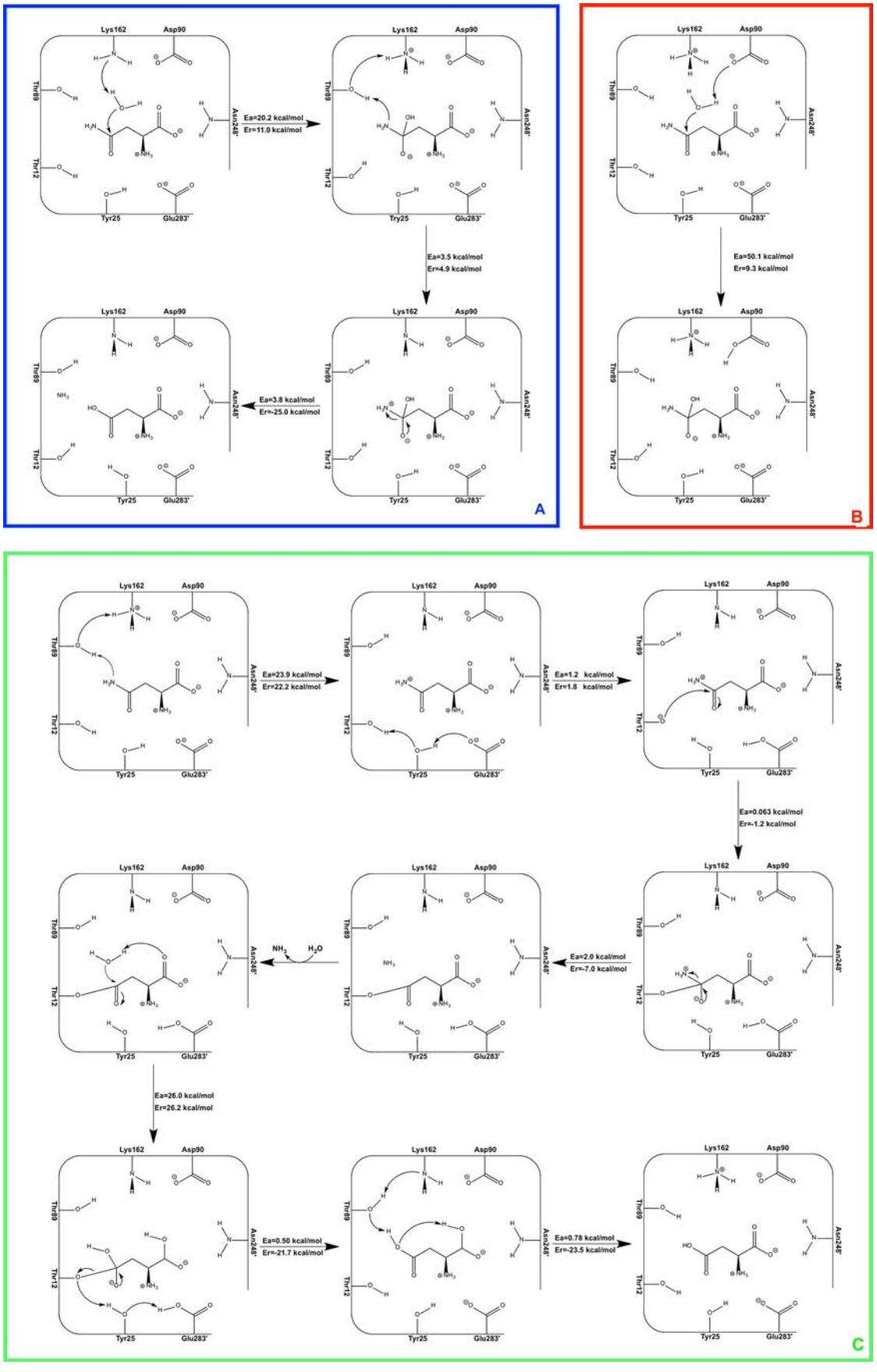

Figure 11. Three reaction pathways (mechanism A, B and C) that were explored by computational means to identify the correct catalytic mechanism of L-asparaginase.

dx.doi.org/10.1021/ja310165u | *J. Am. Chem. Soc.* 2013, 135, 7146−7158

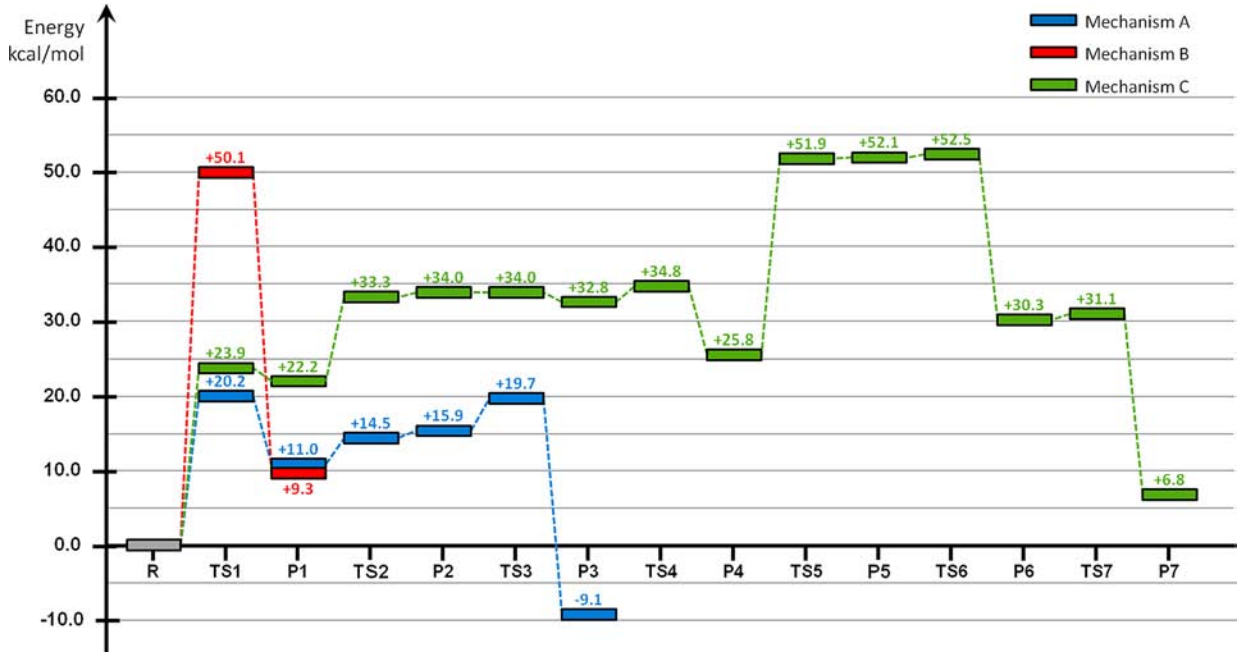

Figure 12. Energetic profile of the three reaction pathways that were explored by computational means to identify the correct catalytic mechanism of L-asparaginase. Mechanism A: Catalytic mechanism with Lys162 in the unprotonated form. Mechanism B: First step of the mechanism A, but with Lys162 in the protonated form. Mechanism C: Mechanism with Lys162 in the protonated form that leads to the formation of the covalent bound adduct between Thr12 and the substrate (the same mechanism occurs when Thr89 is mutated by a valine).

oxygen O4 (−0.69 au), and consequently the tetrahedral intermediate.

Step 3 – Enzymatic Turnover. The last step of the reaction involves the formation of the product of the reaction (glutamate) and the release of one ammonium molecule (Figure 9).

In the optimized geometry of the reactants, it is clear that the interaction between the NH_3 group and carbon C2 of the substrate remains very stable (1.62 Å). The NH_3 and the hydroxyl groups of the substrate side chain interact very closely with two active site residues, Thr89 (1.74 Å) and Lys162 (2.15 Å) respectively, through two hydrogen bonds. In addition, these two residues interact with each other very closely (1.65 Å) through a hydrogen bond, creating a net of hydrogen bonds through which the positive charge of the NH_3 group of the intermediate can spread. Thr12 continues to interact very closely with oxygen O4 of the substrate (1.59 Å) supporting the stability of the tetrahedral intermediate.

In order to trigger the release of ammonia, we scanned the distance between the NH_3 group and carbon C2 of the substrate. The resulting dissociation of an ammonia molecule is very favorable and only has an activation energy of 3.8 kcal/mol. At the transition state it is possible to see that there are two changes occurring simultaneously (Figure 10). As the NH_3 group dissociates from carbon C2 (distance changes from 1.62 to 1.92 Å) forming the aspartate molecule, the distance between oxygen O4 and carbon C2 decreases (1.25 Å), implying the formation of a double bond between both atoms. The hydrogen bonds between Thr89 and Lys162 and between O4 and Thr12 are preserved during the reaction. The transition state structure of this reaction is characterized by an imaginary frequency of 179 icm^{-1}.

At the end of this reaction, the aspartate molecule is generated and the ammonia molecule dissociates from the intermediate. After optimization of the products, the NH_3 molecule is found 4.86 Å away from carbon C2 of the substrate. Carbon C2 and oxygen O4 of the substrate are now connected through a double bond (1.27 Å). The hydroxyl group of Thr12 continues to make a hydrogen bond with oxygen O4 (1.76 Å) as well as Tyr25 (1.70 Å), which turned away from Glu283 in order to interact with it. The full reaction is rather exothermic (−25 kcal/mol), which favors the formation of glutamate.

In the end of these three steps, the reaction is completed and asparaginase can release the aspartate molecule from the active site to the solvent. Subsequently, the protein is ready to take another molecule of asparaginase and start the reaction all over.

Formation of the Acyl-enzyme Intermediate in the Thr89Ala Mutated Enzyme. The results obtained with this study show that the formation of an acyl-intermediate between Thr12 and the substrate is not present in the catalytic process, and therefore should not be present in the natural pathway of the wild-type enzyme (mechanism A of Figure 11). However, there has been a great debate about this intermediate in the literature, mainly because such adduct is found in the mutated X-ray structure 4ECA.[15,17]

It is worth mentioning that we were able to obtain such adduct only when the Lys162 was modeled in the protonated form (mechanism C of Figure 11). The energies involved in some steps of the catalytic pathway were however very high (in the range of the 50 kcal/mol), a condition that turned the full process not feasible at physiological conditions (Figure 12). We tried many other reaction alternatives of the mechanism with Lys162 in the protonated form but with no success due to the high activation energies that were involved in some steps. One of these reactions involved the repetition of mechanism A with Lys162 in the protonated form, but the calculated energies for the first step of the mechanism were already too high, eliminating that pathway as a valid hypothesis (mechanism B of Figure 11 and 12).

dx.doi.org/10.1021/ja310165u | J. Am. Chem. Soc. 2013, 135, 7146−7158

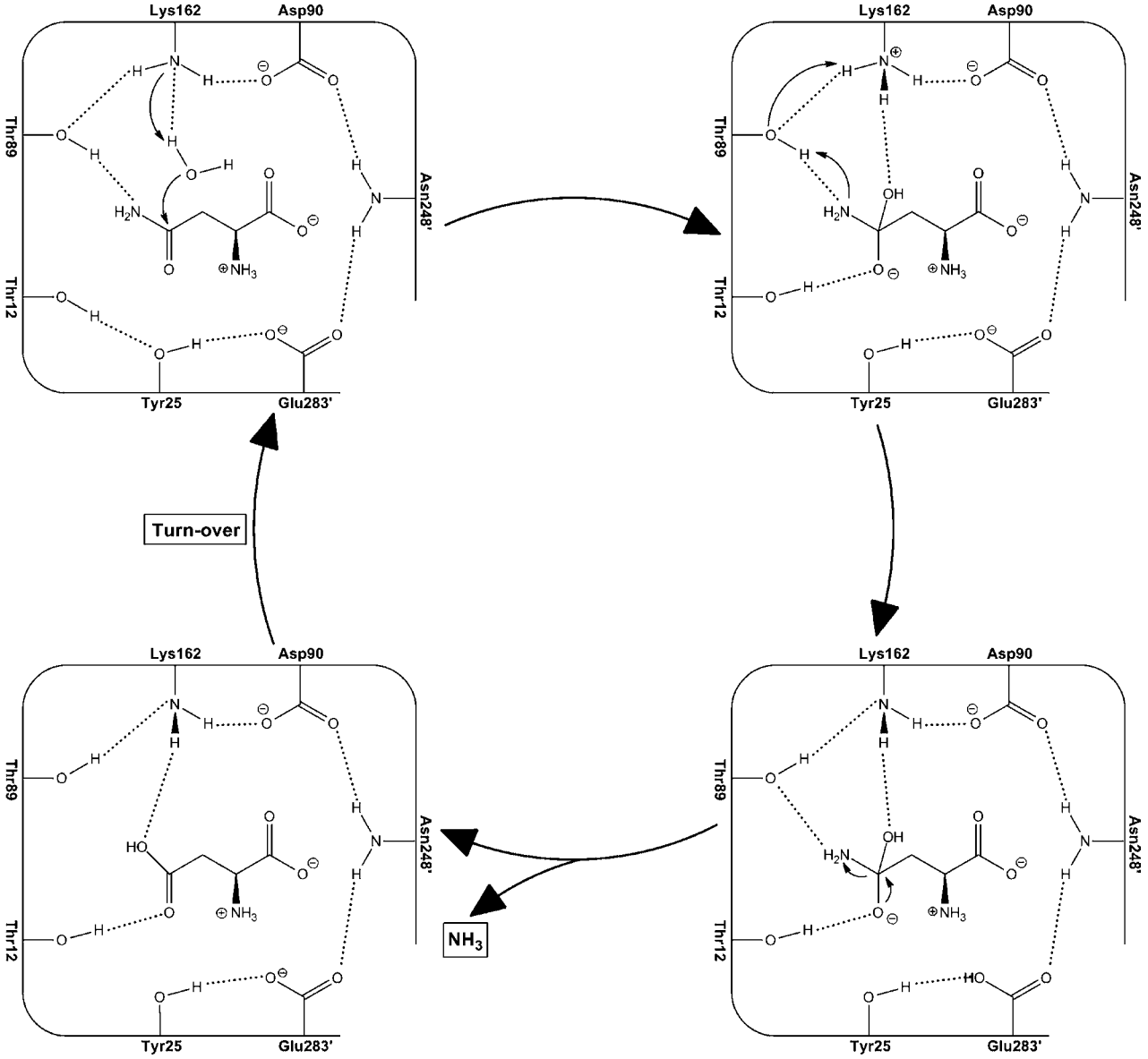

Figure 13. New proposal for the catalytic mechanism of L-asparaginase II.

Taking into account that the covalent adduct between Thr12 and the substrate is only observed when Thr89 is mutated by a valine, we have studied also the same reaction in the presence of such mutation. The optimized geometry of the QM/QM system revealed that the mutation of Thr89 by a valine disrupts the network of hydrogen bonds around Lys162 and the latter moves outward from the active site, similarly to what is observed in the mutated X-ray structure 4ECA that contains such mutation.[17] In spite of these changes, that mechanism is very similar to mechanism C of figure 11 and 12. This occurs because a water molecule, near the active site, occupies the place that is occupied by Thr89 in the wild-type enzyme and plays a similar role (allows the proton transfer between the Lys162 and the substrate). The mechanism then evolves till the formation of the P4 intermediate. When this intermediate is reached, the mechanism comes to a halt due to the high activation energies of the next steps and the absence of Thr89 that is required for the enzymatic turnover. Interestingly, the P4 intermediate corresponds to the state in which the acyl-intermediate with Thr12 is obtained, and from where the mechanism cannot proceed further. This is very consistent with the trapping of the covalent intermediate in the mutated PDB 4ECA structure.

These results show therefore that the formation of the acyl-intermediate with Thr12 is caused by the Thr89Val mutation rather than a true intermediate in the wild-type mechanism. Another piece of evidence that supports this concept is the fact that, when Thr12 is mutated by an alanine, the enzyme becomes less efficient, but remains active (the kcat of the Thr12Ala mutant is approximately 1000 times less than that of the wild-type). Even though one may think that a 1000 fold decrease in the rate constant will render the enzyme completely inactive, in reality this translates in an increase of only 4.2 kcal/mol in the rate-limiting step. It is not strange that the mutation of a residue at the active site, involved in the fundamental H-bond network, destabilizes the TS by 4 kcal/mol and it does not necessarily mean that the residue is participating directly in the reaction but instead that the residue is very close to the reactive center. This suggests that this residue is not an active player in the reaction, as it has been proposed before.[15,17]

dx.doi.org/10.1021/ja310165u | J. Am. Chem. Soc. 2013, 135, 7146−7158

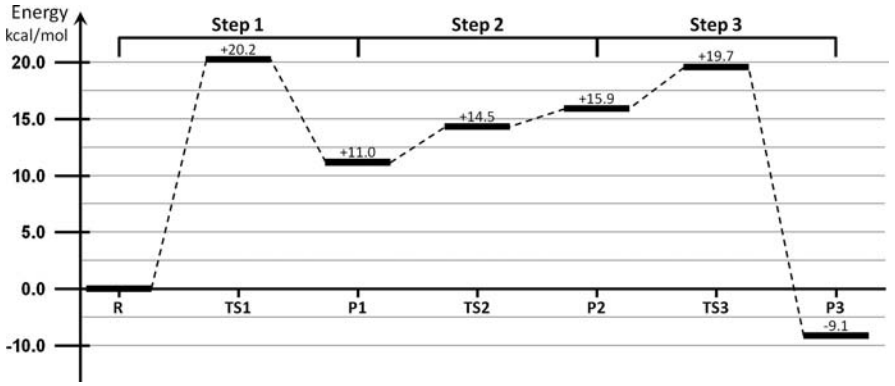

Figure 14. Energetic profile of the catalytic mechanism of L-asparaginase II.

CONCLUSION

The computational results addressed to the study of the catalytic mechanism of L-asparaginase II have shown that the full mechanism involves three sequential steps and requires the nucleophilic attack of a water molecule to the substrate prior to the release of ammonia (Figure 13). The first step of the mechanism involves the formation of a tetrahedral intermediate that results from the nucleophilic attack of the water molecule to carbon C2 of the substrate. In the course of this reaction, Lys162 receives the proton from the water molecule and becomes positively charged. The second step of the reaction involves a concerted double proton transfer from Lys162 to Thr89 and from Thr89 to the substrate, which results in the formation of ammonia. However, the ammonia molecule is still weakly bound to the substrate at this stage. This reaction requires the direct participation of Thr89, which serves as an intermediate in the proton transfer between Lys162 and the substrate. Such configuration is believed to be a result of the stabilization of the tetrahedral intermediate, in which Thr12 and Tyr25 play an active role. The last step of the reaction is very straightforward and involves the dissociation of the ammonia molecule. This reaction is very exothermic, and once it is complete and the product of the reaction leaves the active site, the enzyme is ready for the next turnover. These results also show that the full reaction is almost thermoneutral, a condition that is in agreement with the available experimental results, which show that this enzyme is capable of catalyzing the reaction in both directions (Figure 14).

The results obtained in this papers show that the formation of the acyl-intermediate with Thr12 is a consequence of the Thr89Val mutation rather than a true intermediate in the wild-type mechanism. This suggests that this residue is not an active player on the reaction, as it has been proposed before.[15] However, this does not mean that Thr12 is not important for the catalytic process. Our results show that Thr12, together with Tyr25, is very important for the stabilization of the tetrahedral intermediate that allows the binding of the water molecule to the substrate. If the function of one of these residues is disturbed, as it occurs with the mutation of Thr12 by an alanine, it will slow down the formation of the tetrahedral intermediate. Our conclusions are also supported by the fact that when Thr12 is mutated by a serine, the catalytic activity is not changed. This is completely in line with the catalytic mechanism that we propose. As the role of Thr12 is to stabilize the tetrahedral intermediate and the position the substrate through H-bonding with its side-chain hydroxyl, it becomes obvious that a serine should be able to fulfill the same role with its equivalent hydroxyl group. This is the reason why the catalytic activity is undisturbed in the Thr12Ser mutant. This might explain why the mutation of Thr12 to an Ala makes the enzyme almost inactive, but if it mutated by a Ser residue the normal pathway is maintained.[33]

We believe that the new mechanistic portrait of the catalytic mechanism of L-asparaginase II provides a new, but at the same time complementary, understanding of the catalytic mechanism of L-asparaginases that fully respects all experimental data on this subject. This knowledge is not only important in order to gather an atomistic portrait about the catalytic activity of this enzyme but also to acquire additional information about the transition state structures that are useful to develop new compounds capable of controlling its activity, which is of extreme importance in cancer therapy. As a chemotherapeutic drug, this enzyme can also be harmful to the normal cells in the body if it is active in the bloodstream for a large period of time.[34] For this reason, L-asparaginase therapy is accompanied by the administration of an inhibitor some time after the uptake of the enzyme. With the results we have obtained, new and improved L-asparaginase II inhibitors can be studied.

This knowledge also provides important clues to understand the source of the catalytic activity of the enzyme, which can also be used to enhance its efficiency or modify the type of substrates, or even the reactions that can be catalyzed by these enzymes.

ASSOCIATED CONTENT

Supporting Information

Zip file containing xyz files of the initial model and reactants. This material is available free of charge via the Internet at http://pubs.acs.org.

AUTHOR INFORMATION

Corresponding Author

mjramos@fc.up.pt

Notes

The authors declare no competing financial interest.

ACKNOWLEDGMENTS

The authors would like to thank the financial support provided by FCT (EXCL/QEQ-COM/0394/2012 and grant no. Pest-C/EQB/LA0006/2011).

REFERENCES

(1) Dinndorf, P. A.; Gootenberg, J.; Cohen, M. H.; Keegan, P.; Pazdur, R. *Oncologist* **2007**, *12*, 991.

(2) Verma, N.; Kumar, K.; Kaur, G.; Anand, S. *Crit. Rev. Biotechnol.* **2007**, *27*, 45.
(3) Hill, J. M.; Roberts, J.; Loeb, E.; Khan, A.; MacLellan, A.; Hill, R. W. *J. Am. Med. Assoc.* **1967**, *202*, 882.
(4) Beard, M.; Crowther, D.; Galton, D.; Guyer, R.; Fairley, G. H.; Kay, H.; Knapton, P.; Malpas, J.; Scott, R. B. *Br. Med. J.* **1970**, *1*, 191.
(5) Kobrinsky, N. L.; Sposto, R.; Shah, N. R.; Anderson, J. R.; DeLaat, C.; Morse, M.; Warkentin, P.; Gilchrist, G. S.; Cohen, M. D.; Shina, D. *J. Clin. Oncol.* **2001**, *19*, 2390.
(6) Broome, J. *J. Exp. Med.* **1968**, *127*, 1055.
(7) Ho, P. P. K.; Milikin, E. B.; Bobbitt, J. L.; Grinnan, E. L.; Burck, P. J.; Frank, B. H.; Boeck, L. V. D.; Squires, R. W. *J. Biol. Chem.* **1970**, *245*, 3708.
(8) Ammon, H. L.; Weber, I. T.; Wlodawer, A.; Harrison, R. W.; Gilliland, G. L.; Murphy, K. C.; Sjolin, L.; Roberts, J. *J. Biol. Chem.* **1988**, *263*, 150.
(9) Lubkowski, J.; Wlodawer, A.; Housset, D.; Weber, I. T.; Ammon, H. L.; Murphy, K. C.; Swain, A. L. *Acta Crystallogr., D: Biol. Crystallogr.* **1994**, *50*, 826.
(10) Lubkowski, J.; Palm, G. J.; Gilliland, G. L.; Derst, C.; Rohm, K. H.; Wlodawer, A. *Eur. J. Biochem.* **1996**, *241*, 201.
(11) Swain, A. L.; Jaskolski, M.; Housset, D.; Rao, J. K. M.; Wlodawer, A. *Proc. Natl. Acad. Sci. U.S.A.* **1993**, *90*, 1474.
(12) Miller, M.; Rao, J. K. M.; Wlodawer, A.; Gribskov, M. R. *Febs Lett.* **1993**, *328*, 275.
(13) Aghaiypour, K.; Wlodawer, A.; Lubkowski, J. *Biochemistry* **2001**, *40*, 5655.
(14) Ortlund, E.; Lacount, M. W.; Lewinski, K.; Lebioda, L. *Biochemistry* **2000**, *39*, 1199.
(15) Harms, E.; Wehner, A.; Aung, H. P.; Rohm, K. H. *Febs Lett.* **1991**, *285*, 55.
(16) Derst, C.; Henseling, J.; Rohm, K. H. *Protein Eng.* **1992**, *5*, 785.
(17) Palm, G. J.; Lubkowski, J.; Derst, C.; Schleper, S.; Rohm, K. H.; Wlodawer, A. *Febs Lett.* **1996**, *390*, 211.
(18) Peterson, R. G.; Richards, F. F.; Handschumacher, R. E. *J. Biol. Chem.* **1977**, *252*, 2072.
(19) Derst, C.; Wehner, A.; Specht, V.; Rohm, K. H. *Eur. J. Biochem.* **1994**, *224*, 533.
(20) Dapprich, S.; Komaromi, I.; Byun, K. S.; Morokuma, K.; Frisch, M. J. *J. Mol. Struct.-Theochem* **1999**, *461*, 1.
(21) Morokuma, K.; Froese, R. D.; Dapprich, S.; Komaromi, I.; Khoroshun, D.; Byun, S.; Musaev, D. G.; Emerson, C. L. *Abstr. Pap. Am. Chem. Soc.* **1998**, *215*, U218.
(22) Becke, A. D. *J. Chem. Phys.* **1993**, *98*, 1372.
(23) Lee, C. T.; Yang, W. T.; Parr, R. G. *Phys. Rev. B* **1988**, *37*, 785.
(24) Vosko, S. H.; Wilk, L.; Nusair, M. *Can. J. Phys.* **1980**, *58*, 1200.
(25) Stephens, P. J.; Devlin, F. J.; Chabalowski, C. F.; Frisch, M. J. *J. Phys. Chem.* **1994**, *98*, 11623.
(26) Frisch, M. J.; Trucks, G. W.; Schlegel, H. B.; Scuseria, G. E.; Robb, M. A.; Cheeseman, J. R.; Scalmani, G.; Barone, V.; Mennucci, B.; Petersson, G. A.; Nakatsuji, H.; Caricato, M.; Li, X.; Hratchian, H. P.; Izmaylov, A. F.; Bloino, J.; Zheng, G.; Sonnenberg, J. L.; Hada, M.; Ehara, M.; Toyota, K.; Fukuda, R.; Hasegawa, J.; Ishida, M.; Nakajima, T.; Honda, Y.; Kitao, O.; Nakai, H.; Vreven, T.; Montgomery, J., J. A.; Peralta, J. E.; Ogliaro, F.; Bearpark, M.; Heyd, J. J.; Brothers, E.; Kudin, K. N.; Staroverov, V. N.; Kobayashi, R.; Normand, J.; Raghavachari, K.; Rendell, A.; Burant, J. C.; Iyengar, S. S.; Tomasi, J.; Cossi, M.; Rega, N.; Millam, N. J.; Klene, M.; Knox, J. E.; Cross, J. B.; Bakken, V.; Adamo, C.; Jaramillo, J.; Gomperts, R.; Stratmann, R. E.; Yazyev, O.; Austin, A. J.; Cammi, R.; Pomelli, C.; Ochterski, J. W.; Martin, R. L.; Morokuma, K.; Zakrzewski, V. G.; Voth, G. A.; Salvador, P.; Dannenberg, J. J.; Dapprich, S.; Daniels, A. D.; Farkas, Ö.; Foresman, J. B.; Ortiz, J. V.; Cioslowski, J.; Fox, D. J. *Gaussian 09*; Gaussian, Inc.: Wallingford, CT: 2009.
(27) Cerqueira, N.; Fernandes, P.; Ramos, M. *J. Chem. Theory Comput.* **2011**.
(28) Dewar, M. J. S.; Zoebisch, E. G.; Healy, E. F.; Stewart, J. J. P. *J. Am. Chem. Soc.* **1985**, *107*, 3902.
(29) Zhao, Y.; Truhlar, D. G. *Theor. Chem. Acc.* **2008**, *120*, 215.
(30) Tomasi, J.; Mennucci, B.; Cammi, R. *Chem. Rev.* **2005**, *105*, 2999.
(31) Cerqueira, N. M. F. S. A.; Fernandes, P. A.; Eriksson, L. A.; Ramos, M. J. *Biophys. J.* **2006**, *90*, 2109.
(32) Oliveira, E. F.; Cerqueira, N. M. F. S. A.; Fernandes, P. A.; Ramos, M. J. *J. Am. Chem. Soc.* **2011**, *133*, 15496.
(33) Aghaiypour, K.; Wlodawer, A.; Lubkowski, J. *Biochim. Biophys. Acta* **2001**, *1550*, 117−128.
(34) Aung, H. P.; Bocola, M.; Schleper, S.; Rohm, K. H. *Biochim. Biophys. Acta* **2000**, *1481*, 349.